Original Article

Deep medullary veins: a promising neuroimaging marker for neurodegeneration in multiple sclerosis

Qi Wang[1#^], Ying Shi[1#], Yuan Tian[1], Hongping Chen[2], Jianxiu Lian[3], Jiayun Ren[2], Yuefei Ma[3], Yingzhe Cui[1], Pengfei Liu[1]

[1]Department of Magnetic Resonance, the First Affiliated Hospital of Harbin Medical University, Harbin, China; [2]Department of Neurology, the First Affiliated Hospital of Harbin Medical University, Harbin, China; [3]Philips Healthcare, Beijing, China

Contributions: (I) Conception and design: Q Wang, Y Shi; (II) Administrative support: P Liu; (III) Provision of study materials or patients: H Chen, J Ren; (IV) Collection and assembly of data: Q Wang, Y Shi, Y Cui, Y Tian; (V) Data analysis and interpretation: Q Wang, Y Tian, J Lian, Y Ma; (VI) Manuscript writing: All authors; (VII) Final approval of manuscript: All authors.

[#]These authors contributed equally to this work as co-first authors.

Correspondence to: Pengfei Liu, MD; Yingzhe Cui, MD. Department of Magnetic Resonance, the First Affiliated Hospital of Harbin Medical University, No. 23 Youzheng Street, Nangang District, Harbin 150001, China. Email: liupengfei@hrbmu.edu.cn; 3376@hrbmu.edu.cn.

Background: Multiple sclerosis (MS) is a chronic autoimmune disease of the central nervous system (CNS). Recent studies have shown that different forms of vascular abnormalities may be related to the pathogenesis of MS. Susceptibility-weighted imaging (SWI) can directly image intracranial venules. The aim of this study was to investigate the association between deep medullary veins (DMVs) and the degree of neurodegeneration in patients with MS.

Methods: In this prospective cross-sectional study, 34 patients with MS and 30 age-matched healthy controls (HCs) were recruited. The count and score of DMVs, which can reflect the visibility and continuity of DMVs were evaluated based on SWI. The differences between the group with a high DMV score (DMV >10) and the group with a low DMV score (DMV ≤10) were assessed. The association of DMV change with neurodegeneration neuroimaging markers [including amount and volume of white matter lesion (WML), degree of cortical atrophy, whole-brain atrophy, and deep gray matter (DGM) atrophy] and clinical Expanded Disability Status Scale (EDSS) were observed in patients with MS.

Results: It was found that compared with controls, patients with MS (n=34) had a significantly lower DMV count (P<0.001) and a significantly higher DMV score (P<0.001). The low- and high-DMV score groups differed significantly in terms of EDSS (P=0.048) and neurodegeneration neuroimaging indicators, including WML volume (P=0.015), brain parenchymal fraction (BPF) (P=0.047), thalamic fraction (P=0.036), and caudate fraction (P=0.015). In the correlation analysis of the MS group, DMV count was negatively correlated with the number of WMLs (r=–0.535; P=0.001) and the WML volume (r=–0.416; P=0.014) but positively correlated with the neuroimaging measurements reflecting the degree of whole-brain atrophy and DGM atrophy. Furthermore, the DMV score was positively correlated with EDSS (r=0.450; P=0.008), number of WMLs (r=0.490; P=0.003), and WML volumes (r=0.635; P=0.001) but negatively correlated with the neuroimaging measurements reflecting the degree of whole-brain atrophy and DGM atrophy.

Conclusions: Reduced DMV visibility and continuity could reflect the severity of neurodegeneration in patients with MS. DMV count and score may be imaging indicators for assessing the severity of MS.

^ ORCID: 0009-0002-7197-6046.

Keywords: Multiple sclerosis (MS); deep medullary veins (DMVs); magnetic resonance imaging (MRI); susceptibility-weighted imaging (SWI)

Submitted Jun 04, 2024. Accepted for publication Jan 13, 2025. Published online Feb 26, 2025.
doi: 10.21037/qims-24-1108
View this article at: https://dx.doi.org/10.21037/qims-24-1108

Introduction

Multiple sclerosis (MS) is an immune-mediated inflammatory demyelinating and neurodegenerative disease of the central nervous system (CNS), with relapsing-remitting forms being the most common clinical condition (1,2). MS generally occurs among individuals 20–30 years of age, with a male-to-female ratio of 1:3. Clinical symptoms include sensory deficits, autonomic dysfunction, and ataxia. The etiology and pathogenesis of MS remain unclear, and the risk factors include genetic factors, low vitamin D levels, low sunlight exposure, Epstein-Barr virus infection, and cigarette smoking (3,4). In addition, MS is one of the major disabling diseases among young adults. Unfortunately, there is no cure for immune-mediated attacks on the CNS among patients with MS, and these can result in demyelination and recurring T-cell response (5). Therefore, effectively assessing the severity of the disease and further guiding clinical treatment decisions is critical (6).

Vascular and blood flow disturbances are key elements in pathological process of MS. Evidence of venous involvement in patients with MS can be traced back to the pathological studies of Charcot and Bourneville in the mid-19th century (7-9). In 1916, histologist James W. Dawson was the first to describe periventricular lesions with a finger-like pattern along the central vein, which is now referred to as Dawson's fingers (10). In the 1980s, Adams *et al.* pioneered the demonstration of vasculitis within the walls of the veins and small veins near active MS lesions (11). Recent evidence suggests that vascular components may be the initiating triggers for neuronal pathology and subsequent neurological manifestations of the disease (12).

Magnetic resonance imaging (MRI) is a powerful tool for confirming the diagnosis of MS and monitoring disease progression (13). Conventional MRI has been used to confirm the diagnosis and determine efficacy of disease-modifying therapies (DMTs) via the imaging of new or enlarged lesions (14). Susceptibility-weighted imaging (SWI) has been widely and successfully used for CNS assessment and has become a standard component of most brain MRI protocols. SWI can be considered an upgrade of conventional T2*gradient echo (GRE) sequences since SWI improves the capability of T2*GRE to detect blood and calcium within the CNS (15). Another advantage of SWI is the display of tiny intracerebral veins and the accurate reflection of changes in deoxygenated hemoglobin content (16).

In the examination of deep medullary veins (DMVs), SWI is capable of noninvasively and visually imaging cerebral veins and assessing venous fluid oxygenation (12). SWI is now recognized as a sensitive method for imaging small intracranial veins and is able to visualize DMVs on 3-T MRI (17). However, studies on the correlation between DMVs and neurodegeneration in MS remain limited. There is an urgent need for further attention and research in this area, as clarifying the relationship between cerebral venules and neurodegeneration may provide valuable insights into disease grading and identifying new therapeutic targets.

Therefore, the aim of this study was to assess the changes in the DMVs in patients with MS using SWI, to compare the neuroimaging between groups with low versus high DMV scores, and to determine whether DMV metrics correlate with the neuroimaging markers that reflect neurodegeneration. We present this article in accordance with the STROBE reporting checklist (available at https://qims.amegroups.com/article/view/10.21037/qims-24-1108/rc).

Methods

Participants

Clinical and imaging data of 34 patients with MS admitted to the Department of Neurology of the First Affiliated Hospital of Harbin Medical University between March 2023 and April 2024 were collected.

The inclusion criteria for patients with MS were as follows: (I) diagnosis of definite MS according to the 2017 revised McDonald criteria (18); (II) age >18 years but <60 years without contraindications to 3-T MRI examination; and (III) availability of a 3-T dataset on the same MRI system and standardized MS imaging protocol. Meanwhile,

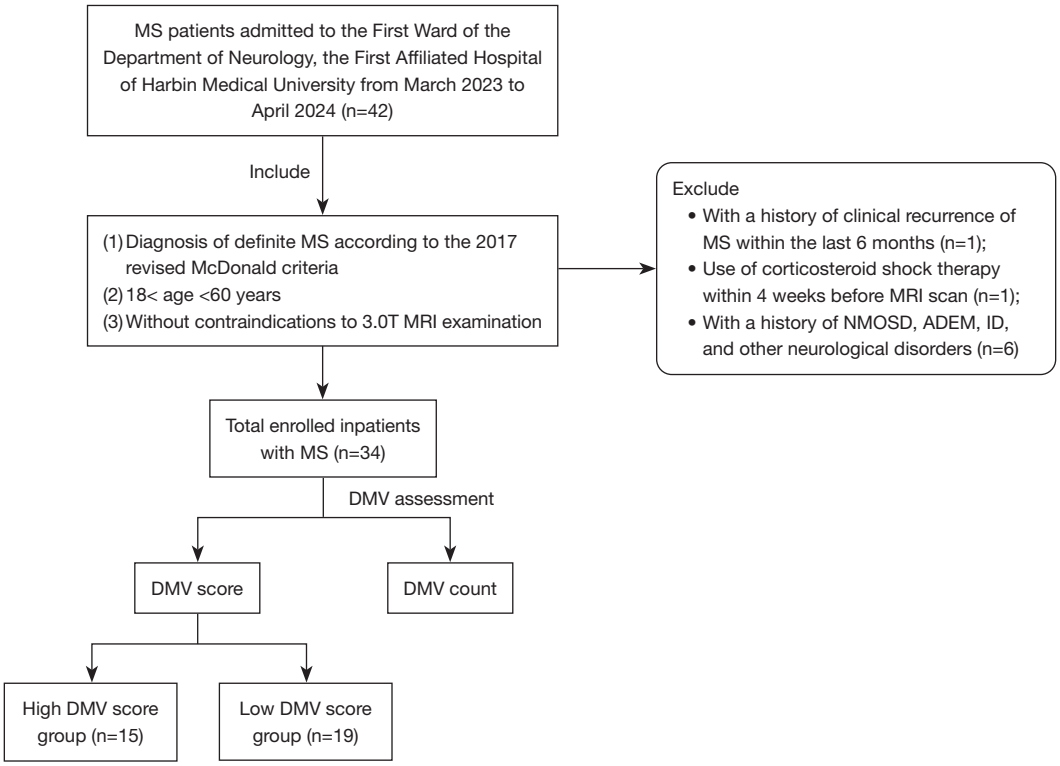

Figure 1 Flowchart of patient enrollment. MS, multiple sclerosis; MRI, magnetic resonance imaging; NMOSD, neuromyelitis optic spectrum disorder; ADEM, acute disseminated encephalomyelitis; ID, idiopathic myelitis; DMV, deep medullary vein.

the exclusion criteria were as follows: (I) patients with a history of clinical recurrence of MS within the previous 6 months; (II) use of corticosteroid shock therapy within 4 weeks prior to the MRI scan (to avoid transient confounding effects of MRI); and (III) patients with a history of neuromyelitis optic spectrum disorder (NMOSD), acute disseminated encephalomyelitis (ADEM), idiopathic myelitis (ID), or other neurological disorders.

Clinical data on the day of MRI examination, such as age, gender, disease duration, and type of DMT were collected from patients. All patients with MS underwent a complete neurological examination and were assessed for overall neurological disability by a trained neurologist using the Expanded Disability Status Scale (EDSS) (19). This study was conducted in accordance with the Declaration of Helsinki (as revised in 2013) and was approved by the Human Research and Ethics Committee of the First Affiliated Hospital of Harbin Medical University (No. 2021JS34). All participants signed informed consent form before participating in the study. The process of enrollment of patients is shown in *Figure 1*.

To compare the imaging data between patients with MS and healthy controls (HCs), 30 age- and sex-matched healthy individuals were recruited during the same period.

Image acquisition

All participants underwent the same whole-brain MRI scanning protocol on a 3-T MR scanner (Ingenia Elition; Philips Healthcare, Best, the Netherlands) with a 32-channel phased-array head coil. The MRI sequence included the following: (I) three-dimensional (3D) T1-weighted imaging (T1WI) [field of view (FOV) =268 mm × 268 mm, matrix =256×256, slice thickness =0.9 mm, time of echo (TE)/time of repetition (TR) =3.1 ms/6.9 ms]; (II) 3D T2-weighted fluid-attenuated inversion recovery (T2-FLAIR) (FOV =268×268 mm, matrix =256 × 256, slice thickness =1.15 mm, TE/TR =3.1/6.9 ms); and (III) SWI performed under a 3D flow-compensated GRE sequence with 100 consecutive layers (slice thickness =2 mm, FOV =230 mm × 180 mm, matrix =576×251, TE/TR =9.8 ms/51 ms). Magnitude and phase images were also acquired.

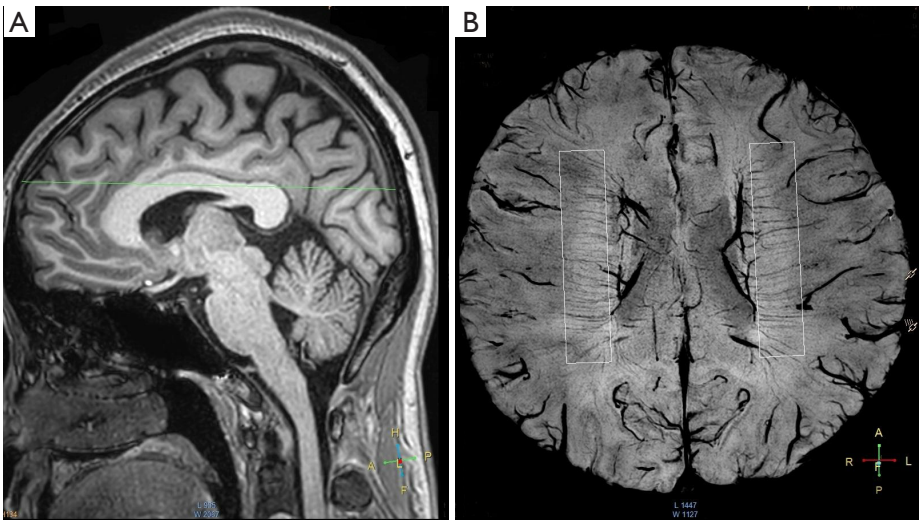

Figure 2 An example of SWI-based assessment of DMV counts in a 32-year-old male. SWI showing normal DMVs. (A) Loss-of-position selection of a 6-mm-thick section parallel to the corpus callosum. (B) Minimum-intensity projection of SWI and DMV count ROI on 3-T MRI. The white rectangular frames represent the ROI placed in the periventricular white matter in each cerebral hemisphere. The DMV count of the patient was 20. SWI, susceptibility-weighted imaging; DMV, deep medullary vein; ROI, region of interest; MRI, magnetic resonance imaging.

DMV assessment

The procedures of DMVs evaluation were divided into two parts: venous visibility and morphological alterations.

(I) The details of the visibility evaluation of DMVs are as follows: the visibility of DMVs on SWI was assessed based on the DMV count according to the method described by Ao *et al.* (17). A two-dimensional (2D) minimum-intensity projection map with a layer thickness of 6 mm was derived from consecutive slices of SWI in the region contoured from the ventricle floor to the superior roof of the corpus callosum (*Figure 2*). Additionally, a region of interest (ROI) of 60 mm × 10 mm was placed in the periventricular white matter (WM) between the frontal and occipital horn in each cerebral hemisphere. Veins that traversed perpendicularly to the lateral ventricular and crossed the ROI were counted via visual inspection, and the number of DMVs was defined as the average count of both hemispheres.

(II) The details of the evaluation for the semiquantitative continuity of DMVs are as follows: evaluation was conducted according to the semiquantitative visual scoring system for DMVs designed by Zhang *et al.* (20). The continuity evaluation was assessed based on the DMV score. DMVs were observed at five consecutive slices of the SWI phase images from the level of the ventricles immediately above the basal ganglia to the level of the ventricles that had immediately disappeared. Based on the anatomical structure of the DMVs, six regions, including the bilateral frontal region, parietal region, and occipital region were separated on the above five slices, and the characteristics of the DMVs were then evaluated in each region, respectively. Separately, the DMVs in each brain region were assessed semiquantitatively and scored according to their continuity and visibility (*Figure 3*). The following four-grade scoring scheme was used for the assessment of DMVs: all DMVs having a continuous and homogeneous signal was scored as 0, at least one DMV with an uneven but continuous signal was scored as 1, at least one DMV with a discontinuous alignment was scored as 2, and no continuous DMVs was scored as 3. The DMV score was calculated by adding together the scores (0 to 3) of the six brain regions. Therefore, the final DMV was scored on a scale of 0–18. Patients were divided into two groups based on the median DMV score: a low-DMV score group and a high-DMV score group.

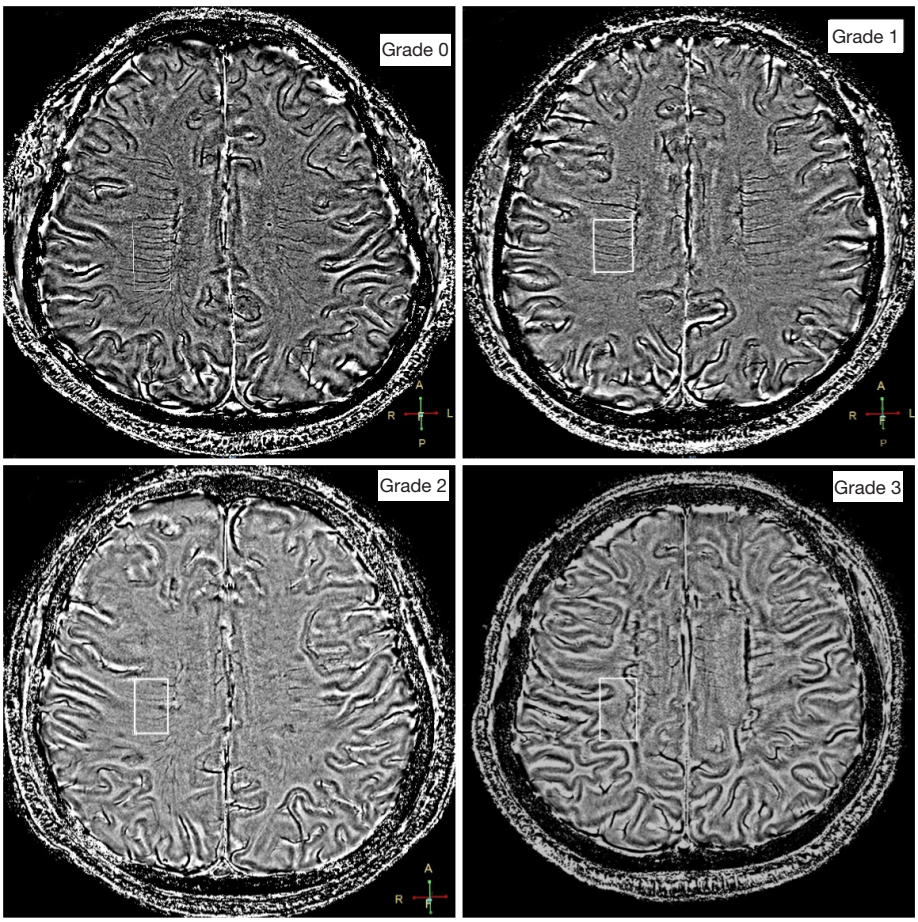

Figure 3 DMV visual score of SWI phase images. An example of the four-point DMV score in parietal region: grade 0, all veins have a continuous and had homogeneous signal; grade 1, all veins are continuous, but one or more veins have an inhomogeneous signal; grade 2, one or more veins are not continuous and have a punctate low signal; and grade 3, no veins are continuous. The white rectangular frames represent the position of the DMV scoring at the right parietal region. DMV, deep medullary vein; SWI, susceptibility-weighted imaging.

Global cerebral image segmentation

Statistical Parametric Mapping 12 (SPM 12) and CAT12 toolbox were run on R2022b MATLAB (MathWorks, Natick, MA, USA) to automatically segment gray matter (GM), WM, and cerebrospinal fluid (CSF) based on 3D T1WI. The scans and segmentation plots of all participants were visually inspected for scan quality (e.g., noise, artifacts, and tissue contrast) and segmentation quality. WM hyperintensities (WMHs) were automatically set to WM mode, which automatically corrects for misclassifications associated with T1 low-signal lesions (21). The 3D T1WI involved surface and thickness estimation and cortical thickness estimation, which were performed using a projection-based thickness method. Total intracranial volume (TIV) was calculated as the sum of GM, WM, and CSF volume. GM fraction (GMF) and WM fraction (WMF) were considered to be the ratios of GM and WM volumes to TIV, respectively. Brain parenchymal fraction (BPF) was the proportion of brain tissue volume equal to the following: (GM + WM)/TIV.

A WM lesion (WML) was defined as an abnormally high signal in periventricular WM or deep WM on T2-FLAIR. The raw data were transferred to the ISP workstation (Intellispace Portal version 10.1, Philips Healthcare) for image postprocessing, in which a semiautomatic edge detection contouring technique based on local thresholding was combined with 3D FLAIR sequences to manually

outline and calculate the WML volume and WML count (the diagnostic criterion was the long axis of the lesion being at least 3 mm in length). The visual manual correction process included the following: (I) the correction of non-WM area being labeled as WML and (II) the correction of the WML area not properly labeled as WML or normal-appearing WM falsely labeled as WML.

Reliability of the radiological assessments

The assessment of all DMV images was performed under double-blind review by two neuroradiologists (Y.S. and Y.C. with 3 and 10 years of experience, respectively) who were completely unaware of the clinical data of the enrolled patients. Furthermore, any disagreements were resolved via discussion with a third neuroradiologist. The intraclass correlation coefficient (ICC) was used to assess the reliability of the DMV counts and DMV score in 10 randomly selected scans.

Statistical analysis

Categorical variables are described as frequencies and percentages, and comparisons between groups were tested with the Chi-squared test. Continuous variables were tested with the Shapiro-Wilk test to verify the normality of data distribution, and normally distributed continuous data are described as mean and standard deviation (SD), with the comparison between groups being tested by the Student *t*-test. Nonnormally distributed data are reported as the median and interquartile range (IQR), with the comparison between groups being tested by the Mann-Whitney tests. The false-discovery rate (FDR) method was used to perform multiple comparison correction. Pearson and Spearman correlation tests were used to determine the correlation between DMVs count/score and number of WMLs, WML volume, whole-brain atrophy, deep GM (DGM) atrophy, and the EDSS in patients with MS. Age and gender were further adjusted for via partial correlation analysis. The final WML volumes were natural log-transformed to normalize skewness. Statistical significance was defined as a two-sided P value <0.05. All statistical analyses were performed with SPSS 26.0 (IBM Corp., Armonk, NY, USA).

Results

Participant characteristics

A total of 34 patients with MS [including 30 with relapse-remitting MS (RRMS) and 4 with secondary progressive MS (SPMS)] (mean age 36.21 years; 79% female) and 30 HCs (mean age 31.57 years; 63% female) were included in this study. The demographic and basic clinical and imaging characteristics of patients with MS and HCs group are summarized in *Table 1* and *Figure 4*. Between patients with MS and HCs, there was no significant difference in gender (P=0.153) or age (P=0.073). The median disease duration in the MS group was 3.25 years, the median EDSS was 1.25, the median number of WMLs was 27, and the mean WML volume was 0.91±0.09.

Visibility and semiquantitative evaluation of DMVs

Compared to the HC group, the MS group had significantly reduced DMV visibility (P<0.001) and significantly higher DMV score (P<0.001). The brain tissue structure segmentation study showed that WMF, GMF, BPF, and cortical thickness were significantly reduced in patients with MS as compared with HCs (all P values <0.001). Moreover, the proportion of DGM structures (including the hippocampus, thalamus, caudate, putamen, and pallidum) in both cerebral hemispheres was significantly reduced in the MS group as compared with the HC group (P<0.001).

The ICCs between the observers were 0.82 for the DMV score and 0.88 for the DMV count.

Clinical and imaging characteristics of patients with MS in the low- and high-DMV score groups

Patients were divided into low- and high-DMV score groups based on a median DMV score of 10. The basic characteristics of patients with MS in the low-DMV score group (DMV score ≤10; IQR, 8–10) and high-DMV score group (DMV score >10; IQR, 11–13) are presented in *Table 2*. Patients with a high DMV score had a higher EDSS (P=0.048) and WML volume (P=0.015). In addition, the high-DMV score group had a lower BPF (P=0.047), thalamus fraction (P=0.036), and caudate fraction (P=0.015). There were no significant differences in age or disease duration between patients with a high DMV score and those with a low score.

Correlation of DMV counts with neuroimaging markers of neurodegeneration

In patients with MS, the DMV count was moderately negatively correlated with the number of WMLs (r=–0.535;

Table 1 Demographic, clinical, and MRI characteristics of patients with MS and HCs

Variables	Patients with MS (n=34)	HCs (n=30)	*t* value/*z* value	Adjusted P value
Gender, female	27 [79]	19 [63]	–	0.153
Age (years)	36.21±1.49	33.5 (25.0, 37.0)	*z*=−2.164	0.073
Disease duration (years)	3.25 (1.00, 8.50)	–	–	–
EDSS	1.25 (0.00, 3.13)	–	–	–
Imaging characteristics				
DMV count	10.97±0.57	14.45±0.60	*t*=−4.224	<0.001**
DMV score	10.00 (8.75, 12.00)	6.50 (4.00, 9.25)	*z*=−4.464	<0.001**
WML count	27 (14, 50.75)	–	–	–
WML volume (mL)	0.91±0.09	–	–	–
Tissue segmentation				
GMF	0.427±0.005	0.464±0.005	*t*=−5.164	<0.001**
WMF	0.329±0.005	0.357 (0.350, 0.365)	*z*=−4.266	<0.001**
BPF	0.756±0.009	0.828 (0.812, 0.847)	*z*=−4.938	<0.001**
Cortical thickness (mm)	2.261±0.016	2.384±0.012	*t*=−5.919	<0.001**
DGM measurements				
Thalamus fraction	0.0050±0.0002	0.0069±0.0001	*t*=−6.620	<0.001**
Hippocampus fraction	0.0041±0.0001	0.0047±0.0001	*t*=−5.600	<0.001**
Caudate fraction	0.0037 (0.0034, 0.0040)	0.0042±0.0001	*z*=−4.314	<0.001**
Putamen fraction	0.0045±0.0001	0.0057±0.0001	*t*=−5.603	<0.001**
Pallidum fraction	0.0002 (0.002, 0.0003)	0.0003 (0.0003, 0.0004)	*z*=−3.075	0.002*

Data are presented as mean ± SD, median (IQR), or n [%]. *, P<0.05, **, P<0.001. The adjusted P value was calculated by the FDR multiple comparison correction method. MRI, magnetic resonance imaging; MS, multiple sclerosis; HC, healthy control; EDSS, Expanded Disability Status Scale; DMV, deep medullary veins; WML, white matter lesion; GMF, gray matter fraction; WMF, white matter fraction; BPF, brain parenchymal fraction; DGM, deep gray matter; SD, standard deviation; IQR, interquartile range; FDR, false-discovery rate.

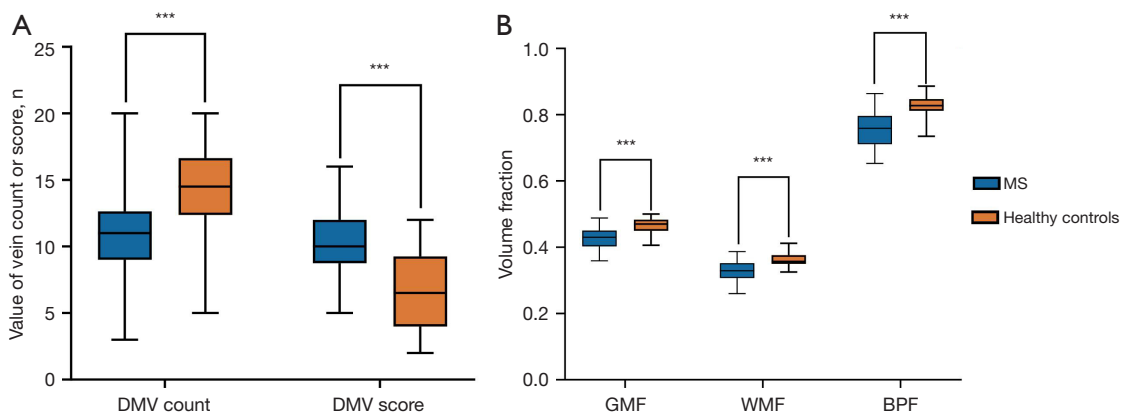

Figure 4 Results of the comparative analysis of 34 patients with MS and 30 HCs. (A) Comparison of DMV count and DMV score between patients with MS and HCs. (B) Comparison of GMF, WMF, and BPF between patients with MS and HCs. ***, P<0.001. MS, multiple sclerosis; HC, healthy control; DMV, deep medullary vein; GMF, gray matter fraction; WMF, white matter fraction; BPF, brain parenchymal fraction.

Table 2 Demographic, clinical, and MRI characteristics of patients with MS in the low- and high-DMV score groups

Variables	DMV score ≤10 (n=19)	DMV score >10 (n=15)	*t* value/*z* value	Adjusted P value
Gender, female	16 [84.2]	11 [73.3]	–	0.503
Age (years)	34.42±2.133	38.47±1.947	*t*=–1.366	0.272
Disease duration (years)	3.00 (1.00, 6.00)	6.00±1.168	*z*=–1.272	0.293
EDSS	1.00 (0.00, 1.50)	2.93±0.603	*z*=–2.421	0.048*
Imaging characteristics				
WML count	26.84±4.580	50.87±8.422	*t*=–2.649	0.050
WML volume (mL)	0.666±0.091	1.218±0.114	*t*=–3.774	0.015*
Tissue segmentation				
GMF	0.436±0.006	0.415±0.009	*t*=1.907	0.11
WMF	0.339±0.007	0.317±0.007	*t*=2.229	0.061
BPF	0.775±0.012	0.732±0.014	*t*=2.360	0.047*
Cortical thickness (mm)	2.279±0.017	2.239±0.029	*t*=1.232	0.283
DGM measurements				
Thalamus fraction	0.0055±0.0003	0.0043±0.0004	*t*=2.632	0.036*
Hippocampus fraction	0.0042±0.0001	0.0041±0.0001	*t*=0.698	0.525
Caudate fraction	0.0039±0.0001	0.0035 (0.0033, 0.0036)	*z*=–3.049	0.015*
Putamen fraction	0.0049±0.0002	0.0040±0.0003	*t*=2.656	0.055
Pallidum fraction	0.0002 (0.0002, 0.0003)	0.0002 (0.0002, 0.0003)	*z*=–0.265	0.811

Data are presented as mean ± SD, median (IQR), or n [%]. *, P<0.05. The adjusted P value was calculated by the FDR multiple comparison correction method. MRI, magnetic resonance imaging; MS, multiple sclerosis; DMV, deep medullary vein; EDSS, Expanded Disability Status Scale; WML, white matter lesion; GMF, gray matter fraction; WMF, white matter fraction; BPF, brain parenchymal fraction; DGM, deep gray matter; SD, standard deviation; IQR, interquartile range; FDR, false-discovery rate.

P=0.001) and WML volume (r=–0.416; P=0.014); DMV count was moderately positively correlated with the WMF (r=0.439; P=0.009) and BPF (r=0.430; P=0.011) but was significantly positively correlated with cortical thickness (r=0.621; P<0.001); DMV count was moderately positively correlated with hippocampal fraction (r=0.470; P=0.005) and caudate fraction (r=0.631; P=0.023) but was significantly positively correlated with thalamus fraction (r=0.730; P<0.001) and putamen fraction (r=0.573; P<0.001). There was no significant correlation between DMV count and EDSS, GMF, or pallidum fraction in patients with MS (all P values >0.05). *Figure 5* shows some of the more significant results of the correlation analysis for DMV count. Age and gender were further adjusted for via partial correlation analysis. *Table 3* shows all the results of the correlation analysis for DMV count.

Correlation between DMV score and neuroimaging markers of neurodegeneration

In the MS group, the DMV score showed a moderate positive correlation with EDSS (r=0.450; P=0.008) and a moderate and significant positive correlation with the number of WMLs (r=0.490; P=0.003) and WML volume (r=0.635; P=0.001). In patients with MS, DMV score had a slight and negative correlation with cortical thickness (r=–0.352; P=0.041) and WMF (r=–0.356; P=0.039); a moderate and negative correlation with BPF (r=–0.427; P=0.012), caudate fraction (r=–0.562; P=0.001), and putamen fraction (r=–0.529; P=0.001); and significant and negative correlation with thalamus fraction (r=–0.615; P<0.001). There was no significant correlation between DMV score and GMF, hippocampus fraction, and pallidum fraction (all P values >0.05). *Figure 5* shows some of the

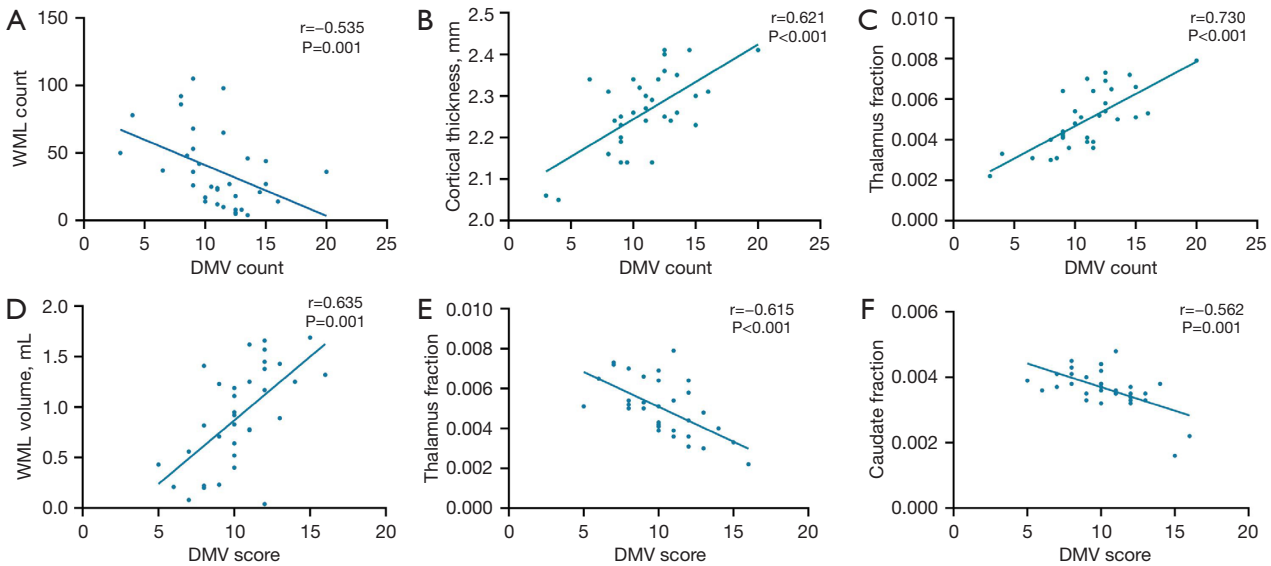

Figure 5 Results of correlation analyses in 34 patients with MS. (A-C) DMV count was negatively correlated with WML count (r=–0.535; P=0.001) and positively correlated with cortical thickness (r=0.621; P<0.001) and thalamus fraction (r=0.730; P<0.001). (D-F) DMV score was positively correlated with WML volume (r=0.635; P=0.001) and negatively correlated with thalamus fraction (r=–0.615; P<0.001) and caudate fraction (r=–0.562; P=0.001). DMV, deep medullary vein; WML, white matter lesion; MS, multiple sclerosis.

Table 3 Correlation analysis of DMV count and score with neuroimaging markers of neurodegeneration and EDSS score in patients with MS

Neuroimaging marker	DMV count		DMV score	
	Correlation	Adjusted correlation†	Correlation	Adjusted correlation†
WML count	–0.535**	–0.504	0.490**	0.513**
WML volume	–0.416*	–0.472	0.635**	0.618**
EDSS	–0.163	–0.370	0.450**	0.445**
GMF	0.332	0.360	–0.336	–0.205
WMF	0.439**	0.456**	–0.356*	–0.405*
BPF	0.430*	0.455**	–0.427*	–0.338
Cortical thickness	0.621**	0.674**	–0.352*	–0.442*
Thalamus fraction	0.730**	0.726**	–0.615**	–0.610**
Hippocampus fraction	0.470**	0.511**	–0.181	–0.114
Caudate fraction	0.631**	0.658**	–0.562**	–0.580**
Putamen fraction	0.573**	0.656**	–0.529**	–0.586**

†, the adjusted correlation results are the partial correlations adjusted for the linear effects of age and sex. *, P<0.05; **, P<0.01. DMV, deep medullary vein; EDSS, Expanded Disability Status Scale; MS, multiple sclerosis; WML, white matter lesion; GMF, gray matter fraction; WMF, white matter fraction; BPF, brain parenchymal fraction.

more significant results of the correlation analysis for DMV score. Age and gender were further adjusted for via partial correlation analysis. *Table 3* shows all the results of the correlation analysis for DMV score.

Discussion

The principal findings of this study were as follows: patients with MS had decreased visibility of DMVs, increased DMV score, and significant brain tissue atrophy and DGM

atrophy as compared to HCs. Among patients with MS, the high-DMV score group had increased WML volume, a higher EDSS, and more pronounced cerebral and DGM atrophy. DMV count or score correlated with neuroimaging markers reflecting the degree of neurodegeneration (WML number and volume; cortical thickness; WMF; BPF; and hippocampus, thalamus, caudate, and putamen fraction) and EDSS.

DMVs are located in the WM, with the vast majority being distributed in the head and body of the caudate nucleus or next to the body of the lateral ventricle, and ultimately drain into the deep venous system via the subventricular veins (16). SWI allows for the detailed visualization of DMVs under noninvasive conditions and does not require the use of exogenous contrast agents. In this study, the evaluation of DMVs was mainly divided into two parts: DMV count was used to evaluate visibility directly, and DMV score was used to evaluate the continuity of DMVs. Given that alterations in the number and continuity of DMVs may reflect different pathological mechanisms (22), we comprehensively assessed DMVs based on the method of counting and scoring DMVs, which has been widely applied in the study of a variety of diseases (17,20,23-25). Visual assessment and several automated segmentation methods have been used in the investigation of cerebral veins. However, when evaluating the DMVs, we adopted the simple and reliable visual counting method due to the regular arrangement of DMVs perpendicular to the ventricles and their minimal anatomical variation. Previous studies have reported reduced visibility of the periventricular WM venous vascular system in patients with MS on SWI (26,27), which remains largely consistent with our findings. Zeng *et al.* also demonstrated that the mean scores of internal cerebral veins (ICVs) and their major tributaries are decreased in patients with MS, with DMVs being progressively diminished and shortened in patients with a longer course of disease (28).

The reduced visibility of DMVs and morphological changes further support the close relationship between MS and vasculature, and we related this observation to other research findings to analyze the causes of altered DMVs in MS. First, diffuse abnormalities of the cerebral veins may be associated with extensive parenchymal injury. The decreased neuronal function, poor oxygen uptake in diseased tissues, and decreased venous deoxygenated hemoglobin level can lead to loss of venous visibility in SWI (26,28) and positron emission tomography (29). Patients with MS have significantly reduced intracerebral oxygen utilization, cortical GM oxygen utilization, and blood flow. Second, proinflammatory cytokines can lead to endothelial dysfunction, increasing the expression of vascular endothelial growth factor and its receptors during the early inflammatory phase of the lesion, promoting the production of vascular adhesion molecules, and ultimately leading to an accelerated inflammatory cycle, loss of neuronal and glial cells, and angiogenesis or remodeling (30).

In our study, there was a statistically significant difference in the volume of periventricular and deep WMLs in patients with MS and high DMV scores as compared to those with low scores. There was a negative correlation between DMV count and WML number and volumes but a positive correlation between DMV score and WML count and volume, which suggests the presence of more severe intracranial lesion loads in patients with more pronounced DMV injury. This is in agreement with the previous findings of Sinnecker *et al.* (31). WML is usually thought to be caused by arteriolar-related injury (32), whereas DMVs are most likely a relatively minor cause of WML generation. The increased WML count and volume in patients with MS may be due to increased local water content resulting from impaired drainage of interstitial fluids or focal inflammatory cellular activity (33). Vos *et al.* (34) found that the abundance of Virchow-Robin spaces containing infiltrating white blood cells was associated with diffuse and focal WM abnormalities on MRI in the autopsy of patients with MS. Gao *et al.* (35) have suggested that venous collagen disease causes venous insufficiency by dilating the veins, leading to vasogenic edema. The pathophysiological changes of venous occlusion are known to lead to increased cerebral venous pressure, accelerated development of interstitial edema, increased CSF production, and decreased absorption and rupture of venous structures (36). In addition, ischemia, which is usually secondary to endothelial dysfunction and impaired autoregulation, leads to impaired drainage of interstitial fluid draining along the perivascular space (35,37), which may also be a principal cause for the increased abundance of WMLs.

It was also found that patients with MS had significantly lower WMF, GMF, BPF, and cortical thickness as compared to HCs; moreover, significant atrophy was found in the DGM of bilateral cerebral hemispheres, which is consistent with some previous studies (38-40). In addition, we associated DMV metrics with brain tissue and subcortical GM morphometry on this basis and found a

positive correlation between DMV count and WMF, BPF, cortical thickness, and the proportion of partial DGM in patients with MS. DMV score was negatively correlated with WMF, BPF, cortical thickness, proportion of partial DGM in patients with MS, indicating that MS brain parenchymal, cortical, and DGM atrophy is most likely associated with DMV damage. In a study in of community cohort comprising 1,056 participants, a lower DMV count was significantly associated with lower GM, WM, and hippocampal volumes (26). However, our results did not indicate a correlation between DMV count and GMF, which could also be due to the relatively small number of patients or the difference in study methods.

The association of local atrophy of the cortex and DGM with damage to the DMVs may be explained by the fact that cerebral atrophy leads to a reduction in brain metabolism, which in turn reduces the level of deoxyhemoglobin in the DMVs. Notably, we also found that thalamic volume reduction exhibited the strongest correlation with altered DMV count and score. There is a growing body of evidence suggesting that the thalamus is one of the most damaged subcortical DGM regions in patients with MS (38,41) and that the atrophy of the subcortical DGM in MS begins in the earliest clinical stages.

To our knowledge, research on the correlation between intracranial small venous injury and brain and DGM atrophy in MS is limited. Our study suggests that reduced visibility and continuity of DMV may be closely associated with early brain atrophy, and subsequent longitudinal studies should be conducted to investigate the temporal relationship and pathophysiological mechanisms related to the changes in DMVs and brain tissue atrophy. In this study, EDSS, which reflects the severity of physical disability in MS, showed a moderately correlation with DMV score, suggesting that DMV impairment may substantially reflect the severity of physical disability in patients with MS.

Certain limitations to this study should be acknowledged. First, as we employed a cross-sectional design, the temporal relationship and causality between DMVs and neurodegeneration in MS could not be determined. Due to the small number of patients with SPMS among the 34 patients with MS, it was not possible to further analyze the differences in DMVs between the SPMS and RRMS populations, and future studies should enroll more patients with other subtypes. Finally, further prospective, large-sample, and multicenter-cohort studies are needed to validate our findings.

Conclusions

This study investigated the association between DMV metrics and neuroimaging markers of neurodegeneration in MS, demonstrating that both DMV count and DMV score may be potential imaging indicators for assessing the severity of brain tissue injury in patients with MS. This may be beneficial for effectively evaluating the severity of the disease and for guiding clinical treatment decisions.

Acknowledgments

None.

Footnote

Reporting Checklist: The authors have completed the STROBE reporting checklist. Available at https://qims.amegroups.com/article/view/10.21037/qims-24-1108/rc

Funding: None.

Conflicts of Interest: All authors have completed the ICMJE uniform disclosure form (available at https://qims.amegroups.com/article/view/10.21037/qims-24-1108/coif). J.L. and Y.M. served as full-time employees of Philips Healthcare during the research period, primarily providing technical support and participating in the revision of the article. The other authors have no conflicts of interest to declare.

Ethical Statement: The authors are accountable for all aspects of the work in ensuring that questions related to the accuracy or integrity of any part of the work are appropriately investigated and resolved. This study was conducted in accordance with the Declaration of Helsinki (as revised in 2013) and was approved by the Human Research and Ethics Committee of the First Affiliated Hospital of Harbin Medical University (No. 2021JS34). All participants signed informed consent form before participation.

References

1. McGinley MP, Goldschmidt CH, Rae-Grant AD. Diagnosis and Treatment of Multiple Sclerosis: A Review. JAMA 2021;325:765-79. Erratum in: JAMA 2021;325:2211.
2. Reeve K, On BI, Havla J, Burns J, Gosteli-Peter MA, Alabsawi A, Alayash Z, Götschi A, Seibold H, Mansmann U, Held U. Prognostic models for predicting clinical disease progression, worsening and activity in people with multiple sclerosis. Cochrane Database Syst Rev 2023;9:CD013606.
3. Marcus R. What Is Multiple Sclerosis? JAMA 2022;328:2078.
4. Volkmann ER, Andréasson K, Smith V. Systemic sclerosis. Lancet 2023;401:304-18.
5. Haque A, Trager NNM, Butler JT, Das A, Zaman V, Banik NL. A novel combination approach to effectively reduce inflammation and neurodegeneration in multiple sclerosis models. Neurochem Int 2024;175:105697.
6. Seifer G, Arun T, Capela C, Laureys G, Jones E, Dominguez-Castro P, Sanchez-de la Rosa R, Hiltl S, Iaffaldano P. Influence of physicians' risk perception on switching treatments between high- efficacy and non-high-efficacy disease-modifying therapies in multiple sclerosis. Mult Scler Relat Disord 2023;76:104770.
7. Haacke EM, Ge Y, Sethi SK, Buch S, Zamboni P. An Overview of Venous Abnormalities Related to the Development of Lesions in Multiple Sclerosis. Front Neurol 2021;12:561458.
8. Bourneville DM, Guérard L. De la sclérose en plaques disséminées. Paris: Delahaye; 1869.
9. Charcot J. Histologie de la sclerose en plaques. Gazette Hôpitaux 1868;41:554.
10. Dawson JW. XVIII.–the histology of disseminated sclerosis. Earth and Environmental Science Transactions of The Royal Society of Edinburgh 1916;50:517-740.
11. Adams CW, Poston RN, Buk SJ, Sidhu YS, Vipond H. Inflammatory vasculitis in multiple sclerosis. J Neurol Sci 1985;69:269-83.
12. Caprio MG, Russo C, Giugliano A, Ragucci M, Mancini M. Vascular disease in patients with multiple sclerosis: a review. J Vasc Med Surg 2016;4:746-53.
13. Kira JI. Redefining use of MRI for patients with multiple sclerosis. Lancet Neurol 2021;20:591-2.
14. Mahajan KR, Ontaneda D. The Role of Advanced Magnetic Resonance Imaging Techniques in Multiple Sclerosis Clinical Trials. Neurotherapeutics 2017;14:905-23.
15. Martín-Noguerol T, Santos-Armentia E, Ramos A, Luna A. An update on susceptibility-weighted imaging in brain gliomas. Eur Radiol 2024;34:6763-75.
16. Li H, Lan Y, Ju R, Zang P. Deep medullary veins as an important imaging indicator of poor prognosis in acute ischemic stroke: a retrospective cohort survey. Quant Imaging Med Surg 2023;13:5141-52.
17. Ao DH, Zhang DD, Zhai FF, Zhang JT, Han F, Li ML, Ni J, Yao M, Zhang SY, Cui LY, Jin ZY, Zhou LX, Zhu YC. Brain deep medullary veins on 3-T MRI in a population-based cohort. J Cereb Blood Flow Metab 2021;41:561-8.
18. Thompson AJ, Banwell BL, Barkhof F, Carroll WM, Coetzee T, Comi G, et al. Diagnosis of multiple sclerosis: 2017 revisions of the McDonald criteria. Lancet Neurol 2018;17:162-73.
19. Kurtzke JF. Rating neurologic impairment in multiple sclerosis: an expanded disability status scale (EDSS). Neurology 1983;33:1444-52.
20. Zhang R, Zhou Y, Yan S, Zhong G, Liu C, Jiaerken Y, Song R, Yu X, Zhang M, Lou M. A Brain Region-Based Deep Medullary Veins Visual Score on Susceptibility Weighted Imaging. Front Aging Neurosci 2017;9:269.
21. Liu ZY, Zhai FF, Ao DH, Han F, Li ML, Zhou L, Ni J, Yao M, Zhang SY, Cui LY, Jin ZY, Zhu YC. Deep medullary veins are associated with widespread brain structural abnormalities. J Cereb Blood Flow Metab 2022;42:997-1006.
22. Nan D, Cheng Y, Feng L, Zhao M, Ma D, Feng J. Potential Mechanism of Venous System for Leukoaraiosis: From post-mortem to in vivo Research. Neurodegener Dis 2019;19:101-8.
23. Xu Z, Li F, Xing D, Song H, Chen J, Duan Y, Yang B. A Novel Imaging Biomarker for Cerebral Small Vessel Disease Associated With Cognitive Impairment: The Deep-Medullary-Veins Score. Front Aging Neurosci 2021;13:720481.
24. Zhang R, Li Q, Zhou Y, Yan S, Zhang M, Lou M. The relationship between deep medullary veins score and the severity and distribution of intracranial microbleeds. Neuroimage Clin 2019;23:101830.
25. Yin X, Han Y, Cao X, Zeng Y, Tang Y, Ding D, Zhang J. Association of deep medullary veins with the neuroimaging burden of cerebral small vessel disease. Quant Imaging Med Surg 2023;13:27-36.
26. Ge Y, Zohrabian VM, Osa EO, Xu J, Jaggi H, Herbert

J, Haacke EM, Grossman RI. Diminished visibility of cerebral venous vasculature in multiple sclerosis by susceptibility-weighted imaging at 3.0 Tesla. J Magn Reson Imaging 2009;29:1190-4.
27. Zivadinov R, Poloni GU, Marr K, Schirda CV, Magnano CR, Carl E, Bergsland N, Hojnacki D, Kennedy C, Beggs CB, Dwyer MG, Weinstock-Guttman B. Decreased brain venous vasculature visibility on susceptibility-weighted imaging venography in patients with multiple sclerosis is related to chronic cerebrospinal venous insufficiency. BMC Neurol 2011;11:128.
28. Zeng C, Chen X, Li Y, Ouyang Y, Lv F, Rumzan R, Wang Z. Cerebral vein changes in relapsing-remitting multiple sclerosis demonstrated by three-dimensional enhanced T_2-weighted angiography at 3.0 T. Eur Radiol 2013;23:869-78.
29. Brooks DJ, Leenders KL, Head G, Marshall J, Legg NJ, Jones T. Studies on regional cerebral oxygen utilisation and cognitive function in multiple sclerosis. J Neurol Neurosurg Psychiatry 1984;47:1182-91.
30. Wardlaw JM, Smith C, Dichgans M. Mechanisms of sporadic cerebral small vessel disease: insights from neuroimaging. Lancet Neurol 2013;12:483-97.
31. Sinnecker T, Bozin I, Dörr J, Pfueller CF, Harms L, Niendorf T, Brandt AU, Paul F, Wuerfel J. Periventricular venous density in multiple sclerosis is inversely associated with T2 lesion count: a 7 Tesla MRI study. Mult Scler 2013;19:316-25.
32. Han H, Ning Z, Yang D, Yu M, Qiao H, Chen S, Chen Z, Li D, Zhang R, Liu G, Zhao X. Associations between cerebral blood flow and progression of white matter hyperintensity in community-dwelling adults: a longitudinal cohort study. Quant Imaging Med Surg 2022;12:4151-65.
33. Wuerfel J, Haertle M, Waiczies H, Tysiak E, Bechmann I, Wernecke KD, Zipp F, Paul F. Perivascular spaces--MRI marker of inflammatory activity in the brain? Brain 2008;131:2332-40.
34. Vos CM, Geurts JJ, Montagne L, van Haastert ES, Bö L, van der Valk P, Barkhof F, de Vries HE. Blood-brain barrier alterations in both focal and diffuse abnormalities on postmortem MRI in multiple sclerosis. Neurobiol Dis 2005;20:953-60.
35. Gao F, van Gaal S, Levy-Cooperman N, Ramirez J, Scott CJM, Bilbao J, Black SE. P2-010: Does variable progression of incidental white matter hyperintensities in Alzheimer's disease relate to venous insufficiency? Alzheimer's & Dementia 2008;4:T368-9.
36. Schaller B, Graf R. Cerebral venous infarction: the pathophysiological concept. Cerebrovasc Dis 2004;18:179-88.
37. Rosenberg GA. Inflammation and white matter damage in vascular cognitive impairment. Stroke 2009;40:S20-3.
38. Houtchens MK, Benedict RH, Killiany R, Sharma J, Jaisani Z, Singh B, Weinstock-Guttman B, Guttmann CR, Bakshi R. Thalamic atrophy and cognition in multiple sclerosis. Neurology 2007;69:1213-23.
39. Steenwijk MD, Daams M, Pouwels PJ, Balk LJ, Tewarie PK, Killestein J, Uitdehaag BM, Geurts JJ, Barkhof F, Vrenken H. What explains gray matter atrophy in long-standing multiple sclerosis? Radiology 2014;272:832-42.
40. Zivadinov R, Heininen-Brown M, Schirda CV, Poloni GU, Bergsland N, Magnano CR, Durfee J, Kennedy C, Carl E, Hagemeier J, Benedict RH, Weinstock-Guttman B, Dwyer MG. Abnormal subcortical deep-gray matter susceptibility-weighted imaging filtered phase measurements in patients with multiple sclerosis: a case-control study. Neuroimage 2012;59:331-9.
41. Rocca MA, Mesaros S, Pagani E, Sormani MP, Comi G, Filippi M. Thalamic damage and long-term progression of disability in multiple sclerosis. Radiology 2010;257:463-9.

Cite this article as: Wang Q, Shi Y, Tian Y, Chen H, Lian J, Ren J, Ma Y, Cui Y, Liu P. Deep medullary veins: a promising neuroimaging marker for neurodegeneration in multiple sclerosis. Quant Imaging Med Surg 2025;15(3):2003-2015. doi: 10.21037/qims-24-1108